Brain Tumor Segmentation from Magnetic Resonance Image using Optimized Thresholded Difference Algorithm and Rough Set

Dalia Mohammad Toufiq [1], Ali Makki Sagheer [2], Hadi Veisi [3]

[1] *University of Sulaimani, College of Medicine, Kirkuk Road, Sulaimania, Iraq*
[2] *Al-Qalam University College, Department of Computer Technical Engineering, Kirkuk, Iraq*
[3] *University of Tehran, Faculty of New Sciences and Technologies,Tehran, Iran*

Abstract **– This research presents an effective method for automatically segmenting brain tumors using the proposed Optimized Thresholded Difference (OTD) and Rough Set Theory (RST). The tumor area is determined using the proposed two-level segmentation algorithm. The first level i.e., an overlay image is created, which is the intensity average of all the pixels of the brain area that were segmented in the initial stage. Then the second level, in which the process of the thresholded difference is applied between the brain area and the overlay image depending on the specified threshold. Features are extracted from the segmented images using the Gray-Level Co-occurrence Matrix (GLCM). To improve performance, an RST is employed with the extracted features. The completely automated methodology is validated using Figshare open dataset.**

Keywords **– Brain tumor segmentation, OTD, GLCM, RST, ID3.**

DOI: 10.18421/TEM112-17
https://doi.org/10.18421/TEM112-17

Corresponding author: Dalia Mohammad Toufiq,
University of Sulaimani, College of Medicine,
Kirkuk Road, Sulaimania, Iraq.
Email: dalia.toufiq@univsul.edu.iq

Received: 16 January 2022.
Revised: 24 March 2022.
Accepted: 30 March 2022.
Published: 27 May 2022.

1. Introduction

A brain tumor is a growth of cells in the brain that is out of control [1]. In the previous several decades, the number of persons dying from a brain tumor has increased. They may be completely removed and do not proliferate after that. Its excellent spatial resolution, tissue contrast, and non-invasive characteristics, magnetic resonance imaging (MRI) are widely used in the medical field [2], [3]. MRI provides useful knowledge for brain tumor diagnosis and treatment [4], [5].

MRI images, nevertheless, are affected by intensity inhomogeneity [6] and weak radiofrequency [7], which might affect the accuracy of the segmentation method. The procedure of brain tumor segmentation involves identifying affected tumor tissues and preserving healthy tissues in the brain by destroying the identified tumor tissues. This task of identifying tumor tissues is carried out in clinical practice using manual annotations. Since manual segmentation requires a lot of time, the development of automated segmentation has been an exciting and important research subject in recent years [8].

To achieve good segmentation results, distortions and artifacts have to be eliminated before the actual segmentation begins. Distortion and artifacts are commonly found in MRI images. While removing such artifacts, it is crucial to keep the essential feature [9], [10], [11], and [12].

One of the segmentation approaches is thresholding, which compares pixel intensities to one or more intensity thresholds. Threshold-based segmentation divides an image into multiple regions depending on the intensity of each pixel [13], [14].

Various feature extraction and classification algorithms were used in traditional methods for disease detection and classification utilizing medical images. Finding the perfect mix of characteristics and a classifier is thought to be a difficult problem. The adoption of GLCM addresses this problem to some extent. Currently, there is a lot of interest in

employing GLCM to implement Computer Aided Diagnosis systems (CAD) [15], [16].

In the classification process, feature selection is crucial, because it greatly reduces computation time and enhances classification accuracy. The use of rough set theory is to identify subsets of attributes that have the same equivalence relation as the complete attribute which is referred to as reduct [17].

Another critical problem is the classification of a brain tumor depending on its classes. Tumors from distinct types, on the other hand, may have similar appearances. This behavior makes the problem more difficult to solve. [2]. A decision tree is a valuable tool in induction research, and it is mostly utilized for model classification and prediction. So far, the ID3 algorithm is the most extensively used decision tree algorithm [18].

Usually, when dealing with tumor segmentation in a brain tumor dataset, the tumors are an area of higher intensity than the rest of the image, so the segmentation process when using thresholding algorithms is to segment the pixels that have a higher intensity than the rest of the image pixels. On the other hand, it may be the other way around, so the segmentation process when using thresholding algorithms is to segment the pixels that are less sharp than the rest of the image pixels.

The Figshare brain tumor data set [19] that is used in this paper, contains contrast-enhanced images with T1 weighting in which the tumor region is in both of the above cases. As a consequence of the convergence of pixel intensities across all brain regions and the lack of high contrast between background and foreground making use of automatic thresholding for segmentation is unhelpful for such a dataset.

In this paper, an Optimized Thresholded Difference (OTD) algorithm is proposed to solve this problem in the process of segmentation of such a data set. The proposed method generates an overlay image first (a uniform intensity gray image, which is the average intensity of all the pixels of the brain image to be segmented), and then the threshold difference between the brain image and the overlay image is applied to extract the tumor regions.

The remainder of this article is arranged as follows: The second section gives a brief overview of related works; The suggested approach is described in depth in Section 3; Section 4 discusses performance measures and the analysis of experimental results, followed by conclusions in section 5.

2. Related Works

As mentioned, several approaches for segmentation have been proposed such as threshold-based, K-means clustering, edge-based, and region growing.

Ivan Cabria et al. in [20] proposed a Potential Field Segmentation (PFS) method that combines the segmentation results of PFS with ensemble techniques. The mass of a pixel is considered as its intensity in this technique, and the potential field for each pixel is calculated. The corresponding pixel is seen as the tumor pixel if the potential field is smaller than the adaptive potential threshold.

Elisee Ilunga-Mbuyamba et al. in [21] proposed a Localized Active Contour Model (LACM). Using this approach, the mean intensity distance between regions of interest and background is automatically balanced. This wants to minimize the active contour's attraction to unwanted borders. It also detects the tumor region using the Hierarchical Centroid Shape Descriptor (HCSD).

Umit Ilhan and colleagues proposed a segmentation approach that clearly distinguishes cancer-affected tumors [22]. This procedure makes the segmented tumor region more visible to the medical practitioner. It employs a variety of techniques, including morphological operations, image filtering, threshold-based segmentation, and pixel subtraction.

Cheng et al. in [23] published the first and the most important research on the classification of brain tumors into a pituitary tumors, meningioma, and glioma based on the Figshare dataset (2015). To extract the ROI, the researchers used tumor masks from the dataset. The ROI was increased by morphological dilations. The augmented ROI was used to extract characteristics such as the bag of words (BOW), GLCM, and the intensity histogram. Different classifiers were evaluated in the experiments. The best results were obtained using a mix of BOW features and a support vector machine (SVM) classifier, resulting in an overall accuracy of 91.28 %.

Ismael and Abdel-Qader suggested a mix of Gabor and Discrete Wavelet Transform (DWT) and a neural network to achieve an accuracy of 91.90 % utilizing Figshare data for the 3-class tumor classification challenge [24].

Swati et al. in [25] suggested using deep transfer learning to classify brain tumors automatically. According to their results, the design utilizing VGG networks exceeded AlexNet in terms of performance. The network's multiple layers were fine-tuned to achieve a classification accuracy of 94.8 %.

Deepak, S., and Ameer, P. M. in [26] propose a technique for classifying medical images using a mix of convolutional neural network (CNN) features and support vector machine (SVM). The completely automated methodology is validated the Figshare open dataset. A five-fold cross-validation procedure was used to review and validate the integrated system. The average classification accuracy of the proposed model was 95.82 %.

3. The Proposed Model

The proposed brain tumor segmentation can be defined in six steps. The process is as follows: Pre-processing, Skull identification and brain region segmentation, Tumor segmentation, Feature extraction, Feature selection (RST), and Classification.

As seen in Figure 1, the first stage is the pre-processing stage. The second and third stage is skull identification and brain region segmentation. To improve the segmentation process, it has been proposed to segment the brain region and separate the skull from it due to its closeness to the intensity of the affected areas in the MRI images. The proposed OTD method was utilized for the segmentation of the affected part from the brain region image.

The Gray Level Co-occurrence Matrix (GLCM) approach is utilized in the fourth step to extract features. The selection of features is the next step. From the features retrieved, the RST approach is suggested for selecting the most relevant features. Finally, the classifier is used to classify the type of tumor as Meningioma, Glioblastoma, and Pituitary gland using the ID3 machine learning mechanism. The details of the method are given in the next sections.

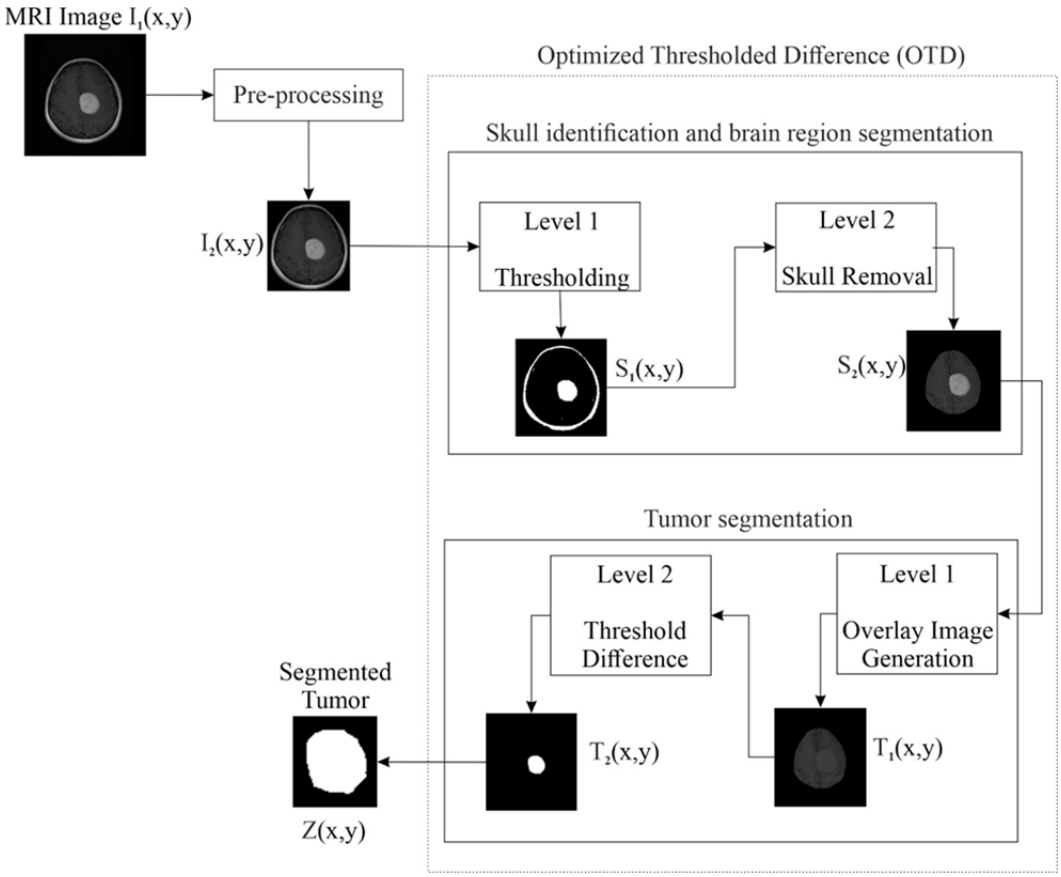

Figure 1. Block diagram of the proposed MRI segmentation model

3.1. Pre-processing

Background minimization tries to reduce non-tumorous region information while preserving tumor-specific features. Here, the background is removed and the brain region is selected using two levels of operations: the first is to determine the starting points for the brain region of the four sides of the image (top, bottom, right, and left). In the second step, the area between the extracted points is truncated and used for the segmentation process.

3.2. Skull Identification and Brain Region Segmentation

Thresholding is a segmentation technique that compares the intensity of a pixel to one or more intensity thresholds. Regarding brain MRI image processing, when using segmentation methods that rely on thresholding methods, the skull bone presents a major challenge in this case. Moreover, it greatly affects the quality of the segmentation process because it has a high intensity comparable to the intensity of the tumor areas in the gray images. Therefore, a method was proposed to remove the bones of the skull and extract the brain region only to

obtain a brain region that does not contain the bones of the skull, so as not to affect later in the process of tumor segmentation.

The proposed removal method consists of two levels:

- The first is the use of the threshold algorithm on an MRI image that results in a binary image (black and white) containing the bones of the skull and some areas affected by the process of applying the threshold. Then, a completed ring is built, which represents the skull ring, depending on the fragmented skull bone areas in the previous step.
- Second, emptying the contents of the resulting ring (in this step we ensure that the process of neglecting the bones of the skull is not accompanied by any neglect of the tumor areas in the brain). The resulting skull ring is adopted as a mask to be applied to the original brain image, in which the areas corresponding to the extracted ring are neglected, and any areas in the original image outside the extracted ring are neglected, and only the area confined in the original image is left inside the extracted ring, which represents the brain region.

3.3. Tumor Segmentation

The proposed Optimized Thresholded Difference OTD algorithm consists of two levels of operation.

In the first level, the brain image resulting from the previous stage is used, where an overlay image is generated, which is a gray image with one intensity, which is the intensity average of all pixels in the brain image. This image is used as an overlay image for the threshold difference process in the second level of the tumor segmentation process.

In the second level, the threshold difference process is applied between the previously segmented brain image and the resulting overlay image from the previous (first) level of the segmentation process. There are several segmented regions in OTD's segmented output. The correct border can be determined by selecting the region with the greatest area. As a result, all regions' perimeters are evaluated, and the region with the largest area is selected as the accurate region.

3.4. Feature Extraction

The GLCM [27] approach was used to extract features from segmented images. It extracts statistical features by evaluating the relationship between *i* and *j* pixels [28]. A set of eight textural features [29], [27] that extracted from each co-occurrence gray level matrix are presented in this paper:

- Entropy:

$$Entropy = \sum_i^M \sum_j^N S_{Img}(\mathrm{i,j}) \log(S_{Img}(i,j)) \quad (1)$$

in which $S_{Img}(\mathrm{i,j})$ is a segmented image.

- Energy:

$$Energy = \sum_i^M \sum_j^N S_{Img}(\mathrm{i,j})^2 \quad (2)$$

- Contrast

$$Contrast = \sum_i^M \sum_j^N |i-j|^2 S_{Img}(i,j)) \quad (3)$$

- Correlation

$$Correlation = \frac{\sum_i^M \sum_j^N (i-\mu_i)(j-\mu_j)}{\sigma_i \sigma_j} \quad (4)$$

The mean and variance are defined by μ and σ respectively.

- Homogeneity (Inverse Difference Moment)

$$Homogeneity = \sum_i^M \sum_j^N \frac{1}{1+(i-j)^2} S_{Img}(i,j) \quad (5)$$

- Variance

$$Variance = \sum_i^M \sum_j^N (i-j)^2 S_{Img}(i,j) \quad (6)$$

- Inverse Difference Moment (IDM):

$$IDM = \sum_{I,j}^{M,N} \frac{S_{Img}(i,j)}{1+|i-j|} \quad (7)$$

- Sum of Square Variance

$$SumofSquareVariance = \sum_i^M \sum_j^N |i-\mu|^2 S_{Img}(i,j)) \quad (8)$$

3.5. Feature Selection

Feature selection has been used to decrease the time of prediction and ignore the features that lead to a false prediction. In data analysis, feature selection utilizing rough set theory is widely used [30]. The rough set theory is utilized to select features in this research.

Information System Table: It can be presented as IST = (U, Att ∪ C) where U is a finite set of objects, Att is a set of an attribute, and C is the decision (class label) [31].

Indiscernibility Relation (*IND* (B)): It is an equivalence relation. Let $a \in A$tt, B ⊆ Att; indiscernibility relation is defined as:

$$\mathrm{IND\ (B)} = \{(x, y) \in U \times U: \forall a \in \mathrm{B},\ a\ (x) = a\ (y)\} \quad (9)$$

Upper approximation of a collection M ($\bar{R}$ (M)) contains all information system table objects that may belong to class M.

The lower approximation of set N ($\underline{R}$ (N)) is the collection of information system table objects that belong to class M.

Positive region refers to the collection of all objects that belong to the lower approximation (Pos(N)).

The boundary region refers to the difference between the upper and lower approximation sets (Bnd(M)).

Equations (10–13) show the mathematical formula for ($\bar{R}$ (M)), ($\underline{R}$ (N)), (Bnd(M)), and (Pos_R(N)):

$$\bar{R}\ (\text{N}) = \{x \in U: R\ (X) \cap x \neq \emptyset\} \quad (10)$$

$$R\ (\text{N}) = \{x \in U: R\ (X) \subseteq x\} \quad (11)$$

$$\text{Bnd(N)} = \bar{\text{R}}\ (\text{N}) - R\ (\text{N}) \quad (12)$$

$$\text{Pos(N)} = \bigcup_{\text{x} \in \frac{\text{U}}{\text{IND(B)}}} R\ (\text{N}) \quad (13)$$

The reduct (Red (R)) is the smallest subset of attributes with the same characteristic as the entire attribute. The overpass of the attributes of reducts is called core (C). The overall number of least subsets of features (S) contending for the reducts becomes

$$S = 2^n - 2 \quad (14)$$

in which n stands for the total number of attributes.

The number of the least subset of attributes produced for every number of attributes (Si) can be calculated by the rule of combination (C). It becomes

$$S_i = C_{\text{n}_i}^N \quad (15)$$

where ni = the number of attributes in the minimal subset.

The following are the processes of choosing the reduct.

Step 1: Find upper approximation of each class utilizing (10);

Step 2: Find a lower approximation of each class by utilizing (11);

Step 3: Compute the positive region of the universe by utilizing (13);

Step 4: Using (14) and (15), determine the number of minimum subsets of attributes;

Step 5: Find indiscernibility of each subset of attributes of a positive region utilizing (9);

Step 6: Compare the indiscernibility of each subset to the attribute's overall indiscernibility;

Step 7: Then choose equivalent indiscernibility as reduct.

3.6. Classification

ID3 is a top-down greedy approach to building a decision tree. It was invented by Ross Quinlan. In simple terms, the top-down strategy indicates that we build the tree from the top-down, whereas the greedy approach means that we choose the best feature at the moment to produce a node at each iteration [32].

Testing and evaluation of the proposed model are followed by fivefold cross-validation procedure. The ID3 model has been trained using the features chosen from the training images, as well as their class labels. The trained ID3 is then given the features derived from testing images. The predicted classes for the testing data are obtained as output from the ID3. The performance of the classifier is assessed by comparing predicted classes with true class labels.

4. Experimental Results

This section contains a comparison of results as well as a discussion. The classifier's performance is assessed and compared to that of related works.

The experimental results for the proposed segmentation method are shown in this section. The data comes from a T1-weighted contrast-enhanced image Figshare database with 233 patient images [19]. As indicated in Table 1, images with an axial view were used in this research with three types of brain tumors: meningioma, glioma, and pituitary tumor.

Table 1. Description of figshare dataset

Type	No of slices
Meningioma	93
Glioma	105
Pituitary tumor	56

Figure 2 shows the output images obtained during preprocessing (background elimination), Skull identification and brain region segmentation (level 1 and level 2), and Tumor segmentation (level 1 and level 2).

4.1. Comparison with Related Works in Terms of Accuracy

Accuracy is expressed as a proportion of true predictions generated by the classifier using Eq (16). All previous work on this specific classification challenge is compared to the proposed method. There are two reasons why classification accuracy is employed as a comparative statistic. In the beginning, it is the standard measure utilized in all related research. Second, the same dataset is used to evaluate the related research. Table 2 summarizes the proposed model performances and gives a performance comparison.

$$\text{Accuracy} = (TP+TN)/(TP+TN+FP+FN) \quad (16)$$

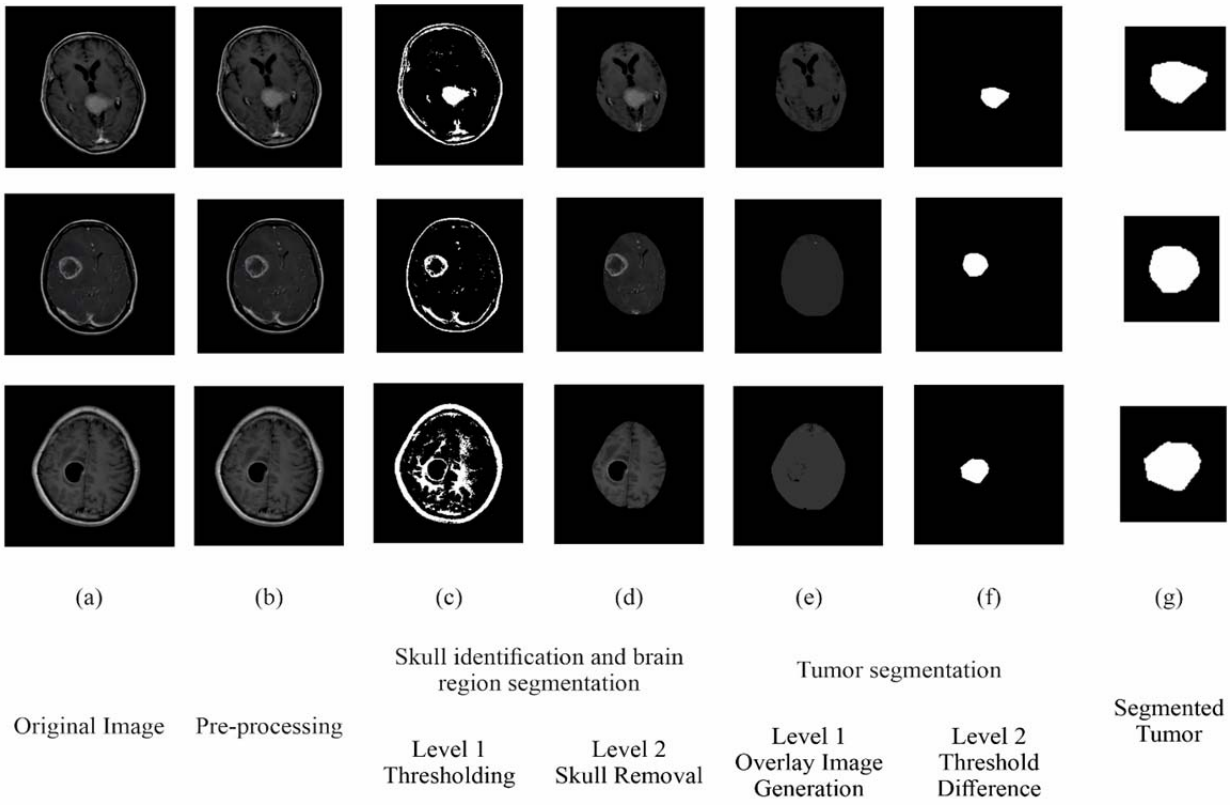

Figure 2. Segmentation of tumor regions outputs: a) Original image, b) Pre-processing, c) Thresholding, d) Skull removal, e) Overlay image generation, f) threshold difference, g) Segmented tumor

Table 2. comparison table of the proposed model with other works

Work	Dataset	Techniques	Accuracy (%)
[24] 2018	Figshare	DWT, Gabor, NN	91.90
[33] 2018	Figshare	CNN, ELM	93.68
[25] 2019	Figshare	CNN (TL)	94.80
[34] 2019	Figshare	DCNN, KNN	98.0
[26] 2020	Figshare	CNN, SVM	95.82
The proposed	Figshare	GLCM, ID3	98.9

4.2. Other Performance Metrics

Since the data set for the category samples is unbalanced, we use a confusion matrix to evaluate the results. The confusion matrix obtained for the experiment is shown in Table 3.

For each class, the following key evaluation metrics are produced using the confusion matrix. For any class (A), Precision (A) is the proportion of samples identified as A that genuinely belong to A. The proportion of actual samples of A that are correctly identified as A is known as recall (A), also known as a classifier's sensitivity. The proportion of non-members of A that are accurately recognized is known as specificity (A). The following are the formulas for calculating the metrics:

$$\text{Precision} = TP/(TP+FP) \quad (17)$$

$$\text{Recall (Sensitivity)} = TP/(TP+FN) \quad (18)$$

$$\text{Specificity} = TN/(TN+FP) \quad (19)$$

Table 4 shows the performance measures for each tumor class. The proposed model is exceptional in terms of specificity across all classes, because it shows the proportion of samples free of a specific tumor class, specificity is an essential statistic in disease categorization. In terms of precision and recall, the classifier is a high-performance model.

Table 3. Confusion matrix of the achieved results

		Actual class			
Predicted class		M	G	P	
	M	92	1	0	M: Meningioma
	G	0	103	1	G: Glioma
	P	1	0	55	P: Pituitary

Table 4. Performance measures for the proposed method

Category	Precision (%)	Recall (%)	Specificity (%)
Meningioma	98.9	98.9	99.4
Glioma	99.0	99.0	99.3
Pituitary tumor	98.2	98.2	99.5

5. Conclusions

This paper is primarily focused on proposing an optimized algorithm for brain tumor segmentation. The proposed Optimized Thresholded Difference (OTD) method consists of two stages, and the first stage is the skull identification and brain region segmentation to improve the segmentation process. It has been proposed to segment the brain region and separate the skull from it due to its closeness to the intensity of the affected areas in the MRI images. The second stage is utilized for the tumor segmentation from the brain region image in two levels; in the first level an overlay image is generated, and then the threshold difference process is applied between the segmented brain image and the overlay image. A set of 8 textural features was obtained from GLCM. Then RST has been used to ignore the features that lead to a false prediction. Finally, ID3 is utilized to perform the classification. In terms of accuracy, precision, recall (specificity), and sensitivity, experimental results demonstrate that the proposed algorithm exceeds the reference approaches.

References

[1]. Gordillo, N., Montseny, E., & Sobrevilla, P. (2013). State of the art survey on MRI brain tumor segmentation. *Magnetic resonance imaging*, *31*(8), 1426-1438.

[2]. Tiwari, A., Srivastava, S., & Pant, M. (2020). Brain tumor segmentation and classification from magnetic resonance images: Review of selected methods from 2014 to 2019. *Pattern Recognition Letters*, *131*, 244-260.

[3]. Maruthamuthu, A. (2020). Brain tumour segmentation from MRI using superpixels based spectral clustering. *Journal of King Saud University-Computer and Information Sciences*, *32*(10), 1182-1193.

[4]. Bauer, S., Wiest, R., Nolte, L. P., & Reyes, M. (2013). A survey of MRI-based medical image analysis for brain tumor studies. *Physics in Medicine & Biology*, *58*(13), R97.

[5]. Li, Y., Jia, F., & Qin, J. (2016). Brain tumor segmentation from multimodal magnetic resonance images via sparse representation. *Artificial intelligence in medicine*, *73*, 1-13.

[6]. Sun, X., Shi, L., Luo, Y., Yang, W., Li, H., Liang, P., ... & Wang, D. (2015). Histogram-based normalization technique on human brain magnetic resonance images from different acquisitions. *Biomedical engineering online*, *14*(1), 1-17.

[7]. Mohan, G., & Subashini, M. M. (2018). MRI based medical image analysis: Survey on brain tumor grade classification. *Biomedical Signal Processing and Control*, *39*, 139-161.

[8]. Naz, S., & Hameed, I. A. (2017, October). Automated techniques for brain tumor segmentation and detection: A review study. In *2017 International Conference on Behavioral, Economic, Socio-cultural Computing (BESC)* (pp. 1-6). IEEE.

[9]. Balasubramanian, G., Chilambuchelvan, A., Vijayan, S., & Gowrison, G. (2016). Probabilistic decision based filter to remove impulse noise using patch else trimmed median. *AEU-International Journal of Electronics and Communications*, *70*(4), 471-481.

[10]. Çalişkan, A., & Çevik, U. (2018). An efficient noisy pixels detection model for CT images using extreme learning machines. *Tehnički vjesnik*, *25*(3), 679-686.

[11]. Chen, Q. Q., Hung, M. H., & Zou, F. (2017). Effective and adaptive algorithm for pepper-and-salt noise removal. *IET Image Processing*, *11*(9), 709-716.

[12]. Gonzalez-Hidalgo, M., Massanet, S., Mir, A., & Ruiz-Aguilera, D. (2018). Improving salt and pepper noise removal using a fuzzy mathematical morphology-based filter. *Applied Soft Computing*, *63*, 167-180.

[13]. Siddiqui, F. U., & Yahya, A. (2022). Introduction to Image Segmentation and Clustering. In *Clustering Techniques for Image Segmentation* (pp. 1-34). Springer, Cham.

[14]. Udupa, P., & Vishwakarma, S. (2016). A survey of MRI segmentation techniques for brain tumor studies. *Bonfring International Journal of Advances in Image Processing*, *6*(3), 22-27.

[15]. Myronenko, A. (2018, September). 3D MRI brain tumor segmentation using autoencoder regularization. In *International MICCAI Brainlesion Workshop* (pp. 311-320). Springer, Cham.

[16]. Preethi, G., & Sornagopal, V. (2014, March). MRI image classification using GLCM texture features. In *2014 international conference on green computing communication and electrical engineering (ICGCCEE)* (pp. 1-6). IEEE.

[17]. Al-Shamery, E. S., & Al-Obaidi, A. A. R. (2018). A New Approach of Rough Set Theory for Feature Selection and Bayes Net Classifier Applied on Heart Disease Dataset. *Journal of University of Babylon for Pure and Applied Sciences*, *26*(2), 15-26.

[18]. Jin, C., De-Lin, L., & Fen-Xiang, M. (2009, July). An improved ID3 decision tree algorithm. In *2009 4th International Conference on Computer Science & Education* (pp. 127-130). IEEE.

[19]. Cheng, J. (2017). Brain tumor dataset. figshare. dataset. Retrieved from: https://doi.org/10.6084/m9.figshare.1512427.v5, [accessed: 25 November 2021].

[20]. Cabria, I., & Gondra, I. (2017). MRI segmentation fusion for brain tumor detection. *Information Fusion*, *36*, 1-9.

[21]. Ilunga-Mbuyamba, E., Avina–Cervantes, J. G., Garcia–Perez, A., de Jesus Romero–Troncoso, R., Aguirre–Ramos, H., Cruz–Aceves, I., & Chalopin, C. (2017). Localized active contour model with background intensity compensation applied on automatic MR brain tumor segmentation. *Neurocomputing*, *220*, 84-97.

[22]. Ilhan, U., & Ilhan, A. (2017). Brain tumor segmentation based on a new threshold approach. *Procedia computer science*, *120*, 580-587.

[23]. Cheng, J., Huang, W., Cao, S., Yang, R., Yang, W., Yun, Z., ... & Feng, Q. (2015). Enhanced performance of brain tumor classification via tumor region augmentation and partition. *PloS one*, *10*(10), e0140381.

[24]. Ismael, M. R., & Abdel-Qader, I. (2018, May). Brain tumor classification via statistical features and back-propagation neural network. In *2018 IEEE international conference on electro/information technology (EIT)* (pp. 0252-0257). IEEE.

[25]. Swati, Z. N. K., Zhao, Q., Kabir, M., Ali, F., Ali, Z., Ahmed, S., & Lu, J. (2019). Brain tumor classification for MR images using transfer learning and fine-tuning. *Computerized Medical Imaging and Graphics*, *75*, 34-46.

[26]. Deepak, S., & Ameer, P. M. (2021). Automated categorization of brain tumor from mri using cnn features and svm. *Journal of Ambient Intelligence and Humanized Computing*, *12*(8), 8357-8369

[27]. Haralick, R. M., Shanmugam, K., & Dinstein, I. H. (1973). Textural features for image classification. *IEEE Transactions on systems, man, and cybernetics*, (6), 610-621.

[28]. Badža, M. M., & Barjaktarović, M. Č. (2021). Segmentation of Brain Tumors from MRI Images Using Convolutional Autoencoder. *Applied Sciences*, *11*(9), 4317.

[29]. Aborisade, D. O., Ojo, J. A., Amole, A. O., & Durodola, A. O. (2014). Comparative analysis of textural features derived from GLCM for ultrasound liver image classification. *Energy*, *2*(10).

[30]. Nahato, K. B., Harichandran, K. N., & Arputharaj, K. (2015). Knowledge mining from clinical datasets using rough sets and backpropagation neural network. *Computational and mathematical methods in medicine*, *2015*.

[31]. Pawlak, Z., & Skowron, A. (2007). Rudiments of rough sets. *Information sciences*, *177*(1), 3-27.

[32]. Quinlan, J. R. (1986). Induction of decision trees. *Machine learning*, *1*(1), 81-106.

[33]. Pashaei, A., Sajedi, H., & Jazayeri, N. (2018, October). Brain tumor classification via convolutional neural network and extreme learning machines. In *2018 8th International conference on computer and knowledge engineering (ICCKE)* (pp. 314-319). IEEE.

[34]. Deepak, S., & Ameer, P. M. (2019). Brain tumor classification using deep CNN features via transfer learning. *Computers in biology and medicine*, *111*, 103345.